Admittance of metal–insulator–semiconductor tunnel contacts in the presence of donor–acceptor mixed interface states and interface reaction

P. Chattopadhyay

Citation: Journal of Applied Physics **89**, 364 (2001); doi: 10.1063/1.1324692
View online: http://dx.doi.org/10.1063/1.1324692
View Table of Contents: http://scitation.aip.org/content/aip/journal/jap/89/1?ver=pdfcov
Published by the AIP Publishing

Admittance of metal–insulator–semiconductor tunnel contacts in the presence of donor–acceptor mixed interface states and interface reaction

P. Chattopadhyay
Department of Electronic Science, University College of Science, 92, Acharyya Prafulla Chandra Road, Calcutta-700 009, India

(Received 31 May 2000; accepted for publication 19 September 2000)

The admittance of a metal–insulator–semiconductor tunnel contact is evaluated considering the presence of donor–acceptor mixed interface states and chemical reaction in the interfacial oxide layer. Both the voltage and frequency behavior of the device has been studied. It has been found that, due to interface reaction, the current, conductance, and capacitance of the device drift considerably with time yielding an aging effect. Further, it is revealed that the dependence of the conductance and capacitance on the aging time stem rapidly from changing time constants of the interface states with aging time. The results are discussed with special reference to well known admittance spectroscopy used for the characterization of interface states. © *2001 American Institute of Physics.* [DOI: 10.1063/1.1324692]

I. INTRODUCTION

Interface states play a crucial role on the electrical characteristics of metal–semiconductor (MS) and metal–insulator–semiconductor (MIS) tunnel devices.[1–19] The fixation of Fermi level,[1–4] the deviation of the device quality factor from unity,[5] and the frequency dispersion of the conductance and capacitance of the device[6,13,16,17] are the direct manifestations of interface state effects in these devices. There are, however, different opinions in modeling MS or MIS interfaces. Among these, the description in terms of acceptor states is well known.[1–5] The acceptor states may appear intrinsically at the surface or as a result of extension of the wave function of the metal atoms up to the semiconductor creating metal induced gap states.[20,21] These states are known to be responsible for the so-called surface pinning effect. However, the existence of donor states at low metal coverage cannot be ruled out.[22] There are also apprehensions of donor-like defects extended in to the semiconductor regions caused by sputtering.[23,24] The description of interface in terms of acceptor states has been used to develop admittance models for MIS tunnel devices.[6,13,16,17] According to the original admittance model,[25] the interface state conductance and the capacitance are frequency dependent due to relaxation processes at interface states determined by the time constant of these states. So long as only one variety of states exists at the interface, the conductance peak in the frequency domain relates the parameters that characterize the states. However, in a number of experiments with Schottky barriers or metal–oxide–semiconductor structures, the observed conductance plots have been found to exhibit a number of peaks that can be attributed to multilevel deep traps[26,27] or deep levels in association with interface states.[28,29] Recent developments in this field further reveal that the description of MIS interface only in terms of interface states is inadequate. It has been shown that the device properties may be greatly influenced by interface reaction and the device may show the aging effect.[30,31] It has been shown that the chemical reaction of the metal contact with the adjacent SiO_2 layer yields fourfold silicon traps capable of accepting electrons and thereby causing a negative charge buildup in the interfacial layer.[31] Consequently, the barrier height of the device becomes dependent on time. The interface reaction is particularly important for various silicon devices.[32,33] The role of interfacial SiO_2 on the electrical characteristics of metal–semiconductor and related devices has been reviewed very recently.[34]

The objective of the present work is to discuss the consequences of donor–acceptor mixed interface and interfacial reaction on the admittance of MIS tunnel devices. It is shown that a description in terms of a donor–acceptor composite at the interface offers an alternative explanation for the observed distortion in the admittance plots and further that such plots drift with time due to the chemical reaction of metal with the interfacial insulating layer, thereby resulting in the aging effect in these devices. In Sec. II of this article, the basic equations necessary to evaluate dc behavior of the device are presented. The interface state model considered in this work is discussed in Sec. III. The response of the device under ac conditions is discussed in Sec. IV followed by the evaluation of the device admittance in Sec. V. The effect of the interface reaction of the admittance plots has been addressed in Sec. VI. Finally, the results arrived at are critically discussed with special reference to admittance spectroscopy for the characterization of interface states in Sec. VII.

II. BASIC EQUATIONS

The energy band diagram of a metal–semiconductor system with thin interfacial oxide layer and in the presence of an applied voltage V is shown in Fig. 1. The oxide layer may be present inherently on the semiconductor surface before the metal deposition and, therefore, its effect should be considered for generality. In the band diagram ϕ_m is the work function of the metal, δ the thickness of the oxide layer, χ the electron affinity of the semiconductor, V_i the potential

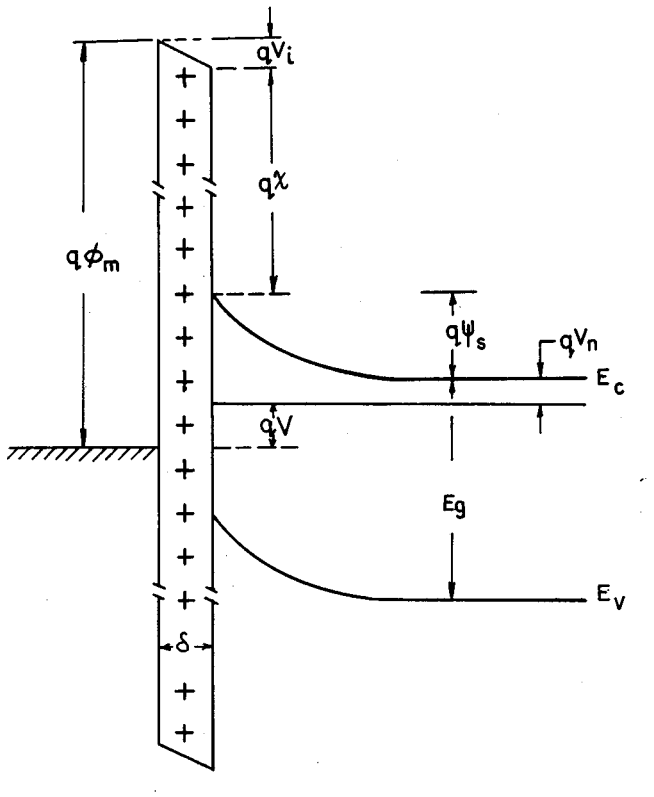

FIG. 1. Energy band diagram of a MIS tunnel contact.

drop across the interfacial layer, ψ_s the surface potential, positive signs represent fixed charges in the interfacial layer, and other terms have their usual meaning. The charge density in the interfacial layer may be positive or negative. In the case of silicon devices with SiO_2 acting as the interfacial layer, the fixed charges have been found to be positive,[13] while the oxide on GaAs has been found to posses a negative charge density.[10] Therefore, depending on the oxide used, a proper sign for the fixed charges has to be considered. We will restrict this analysis for silicon devices having a native SiO_2 interfacial layer and choose the fixed charge density to be positive. The analysis can be made applicable for devices on GaAs by merely changing the sign of the charge. The dc behavior of the device can be evaluated considering the formulation originally developed by Cowley and Sze[3] may be modified in the presence of external dc bias V.

The charge neutrality equation for a metal–semiconductor system with a thin interfacial oxide layer can be written as

$$Q_m+Q_{\rm sc}+Q_{\rm it}+Q_f=0, \tag{1}$$

where $Q_{\rm sc}$ represents semiconductor space charge density, $Q_{\rm it}$ the charge density trapped at the interface, Q_f the fixed charge density, and Q_m is the charge density that appears in the metal.

The potential drop across the interfacial layer can be obtained using Gauss's law [2]

$$V_i=-\delta Q_m/\epsilon_i, \tag{2}$$

where ϵ_i is the permittivity of the interfacial layer.

One can also obtain V_i from the energy band diagram given by

$$V_i=\phi_m-\chi-\psi_s-V_n-V. \tag{3}$$

Eliminating V_i using Eqs. (2) and (3), one obtains

$$\phi_m-\chi-\psi_s-V_n=\delta/\epsilon_i[Q_{\rm sc}+Q_{\rm it}+Q_f]. \tag{4}$$

Now, the depletion layer charge density is given by

$$Q_{\rm sc}=(2q\epsilon_s N_D\psi_s)^{1/2}, \tag{5}$$

where ϵ_s is the permittivity of the semiconductor and N_D is the doping concentration. Equation (4) can be solved for the surface potential with the help of Eq. (5) and the proper interface state model. The results can be used for the analyses of the current density, conductance, and capacitance of the device.

III. INTERFACE STATE MODEL AND SURFACE POTENTIAL

A number of possibilities may be considered for the evaluation of trapped charge density at the metal–semiconductor interface. First, the interface states may be all acceptorlike. This case refers to devices having an ultrathin interfacial oxide layer, e.g., the devices fabricated on vacuum cleaved and chemically cleaned surfaces.[4] A second choice being the donor states at the oxide–semiconductor interface. Third, there could be a mixed interface composed of both donor and acceptor states. The above three possibilities may be discussed as three different cases, namely, when the interface states are (i) all acceptorlike, (ii) all donorlike, and (iii) a composite of donors and acceptors.

Case 1: *Interface states are all acceptorlike and distributed throughout the band gap.*

In this case, the charge density at the interface states will be determined by the position of the Fermi level relative to the valence band edge at the surface. From the band diagram

$$Q^a_{\rm it}=-q\int_0^{\infty} D^a_{\rm it}(E)F(E)dE$$

$$=-q\int_0^{E_{\rm fs}} D^a_{\rm it}(E)F(E)dE-\int_{E_{\rm fs}}^{\infty} D^a_{\rm it}(E)F(E)dE, \tag{6}$$

where $D^a_{\rm it}(E)$ is the density of interface states and $F(E)$ is the probability of occupation. The superscript ''a'' stands for acceptor-like states. The second term in Eq. (6) actually accounts for the contribution of interface trapped charge density due to extension of $F(E)$ above $E_{\rm fs}$. As the contribution of this term is negligible compared to the first term in Eq. (6), the interface trapped charge density can be approximated as

$$Q^a_{\rm it}=-q\int_0^{E_{\rm fs}} D^a_{\rm it}(E)d(E). \tag{7}$$

With $E_{\rm fs}=q\psi_s+qV_n$ and constant interface state density, one obtains from Eqs. (4), (5), and (7),

$$\phi_m-\chi-\psi_s-V_n-V=\delta[(2q\epsilon_s N_D\psi_s)^{1/2}-q^2D^a{}_{\rm it}\times(E_g-q\psi_s-qVn)+qN_f]/\epsilon_i, \tag{8}$$

where $Q_f=qN_f$ is substituted, N_f being the density of interface fixed charges per cm^2 in the oxide. The surface potential ψ_s can be readily solved from Eq. (8) given by

$$\psi_s=C_{2a}(\phi_m-\chi)+(1-C_{2a})E_g-C_{2a}qN_f\delta/\epsilon_i-C_{2a}V-V_n+(C_{2a}^2C_1)/2-[4\{C_{2a}(\phi_m-\chi)+(1-C_{2a})E_g-C_{2a}q\delta N_f/\epsilon_i-C_{2a}V-V_n\}C_{2a}^2C_1+C_{2a}^4C_1^2]^{1/2}/2, \tag{9}$$

where $C_{2a}=\epsilon_i/(\epsilon_i+q^2\delta D_{\rm it}^q)$ and $C_1=(2q\epsilon_sN_D\delta^2)/\epsilon_i^2$.

Case 2: *Interface states are donorlike and distributed throughout the band gap.*

The charge density at the interface states in this case is determined by the number of unoccupied states above the Fermi level given by

$$Q_{\rm it}^d=q\int_{E_{\rm fs}}^{E_g}D_{\rm it}^d(E)[1-F(E)]dE. \tag{10}$$

Assuming that the states above $E_{\rm fs}$ are all empty, then Eq. (10) can be approximated as

$$Q_{\rm it}^d\cong q^2D_{\rm it}^d(q\psi_s+qV_n). \tag{11}$$

From Eqs. (4), (5), and (11) one obtains

$$\phi_m-\chi-\psi_s-V_n-V=\delta[(2q\epsilon_sN_D\psi_s)^{1/2}+q^2D_{\rm it}^d(q\psi_s+qV_n)+qN_f]/\epsilon_i. \tag{12}$$

Equation (12) can be solved for the surface potential given by

$$\psi_s=C_{2d}(\phi_m-\chi)-C_{2d}q\delta N_f/\epsilon_i-V_n-C_{2d}V+C_{2d}^2C_1/2-[4\{C_{2d}(\phi_m-\chi)-C_{2d}V-V_n-C_{2d}q\delta N_f/\epsilon_i\}\times C_{2d}^2C_1+C_{2d}^4C_1^2]^{1/2}/2, \tag{13}$$

where $C_{2d}=\epsilon_i/(\epsilon_i+q^2\delta D_{\rm it}^d)$.

Case 3: *Donor–acceptor composite interface.*

This case refers to a positive interface state trapped charge density resulting from the empty donor states above the Fermi level in addition to the negative charge density at the acceptor states below the Fermi level. The net charge density at the interface states is therefore given by

$$Q_{\rm it}=Q_{\rm it}^a+Q_{\rm it}^d=-q\int_0^{E_{f_s}}D_{\rm it}^aF(E)dE+q\int_{E_{f_s}}^{E_g}D_{\rm it}^d[1-F(E)]dE. \tag{14}$$

Considering the contribution of $F(E)$ to be negligible above $E_{\rm fs}$, one obtains from Eq. (14)

$$Q_{\rm it}=-qD_{\rm it}^a(E_g-\psi_s-qV_n)+qD_{\rm it}^d(q\psi_s+qV_n). \tag{15}$$

On substituting Eqs. (5) and (15) into Eq. (4), one obtains

$$\phi_m-\chi-\psi_s-V_n-V=\delta[(2q\epsilon_sN_D\psi_s)^{1/2}+q^2\times(D_{\rm it}^a+D_{\rm it}^d)\psi_s+q^2(D_{\rm it}^a+D_{\rm it}^d)\times V_n-q^2D_{\rm it}^aE_g+qN_f]/\epsilon_i. \tag{16}$$

Equation (16) can be solved for ψ_s given by

$$\psi_s=\psi_{ad}/\{C_{2d}+(1-C_{2d})C_{2a}\}+C_{2a}^2C_{2d}^2C_1/[2\{C_{2d}+(1-C_{2d})C_{2a}\}]^2-[4C_{2a}^2C_{2d}^2C_1\psi_{ad}\times\{C_{2d}+(1-C_{2d})C_{2a}\}+C_{2a}^4C_{2d}^4C_1^2]^{1/2}/[2\{C_{2d}+(1-C_{2d})C_{2a}\}]^2, \tag{17}$$

where

$$\psi_{ad}=C_{2a}C_{2d}(\phi_m-\chi)+(1-C_{2a})C_{2d}E_g-qC_{2a}C_{2d}\delta N_f/\epsilon_i-\{C_{2d}+(1-C_{2d})C_{2a}\}V_n-C_{2a}C_{2d}V.$$

It can be verified that Eq. (17) converges to Eqs. (9) and (13) in the limits $D_{\rm it}^a\to0$ and $D_{\rm it}^d\to0$, respectively.

IV. RESPONSE UNDER ac CONDITIONS

The ac behavior of a given metal–semiconductor system with a thin interfacial oxide depends primarily on two mechanisms. First, under a small signal ac condition, the surface potential fluctuates and thereby modulates the tunnel current.[16] A second mechanism being trapping–detrapping of carriers at the interface states described by Schokley–Read–Hall statistics.[25] The charging and discharging current in the semiconductor may be considered as a third current component under ac condition.[25]

In order to obtain the ac component of the tunnel current, one may start with the basic current–voltage relation of MIS tunnel diodes. Assuming the transverse momenta of the carriers are conserved during tunneling, an expression for current density across the diode can be derived given by[3]

$$J_{\rm dc}=A^*T^2\exp[(-\phi^{1/2}\delta)]\exp[-q(\psi_s+qV_n)/kT], \tag{18}$$

where $\exp[(-\phi^{1/2}\delta)]$ represents a tunneling attenuation factor, ϕ the oxide mean barrier, δ the thickness of the insulating layer, and the other terms have their usual meaning. Now, if a small signal ac voltage is applied in addition to the dc voltage, there will be an ac fluctuation in the surface potential, $\delta\psi_s$. The ac tunnel current has been derived by Werner[16] by considering the variation $\delta\psi_s$ to be small given by

$$J_{\rm ac+dc}=\theta A^*T^2[\exp-(q\psi_s/kT)][1+(q\delta\psi_s/kT)]=J_{\rm dc}[1+(q\delta\psi_s/kT)], \tag{19}$$

where the terms $\exp[(-\phi^{1/2}\delta)]$ and $\exp[-(qV_n/kT)]$ are absorbed in the parameter θ. The ac tunnel current can be directly obtained from Eq. (19) given by

$$j_{\rm ac}=J_{\rm ac+dc}-J_{\rm dc}=J_{\rm dc}\delta\psi_s/kT. \tag{20}$$

The current resulting from the charging and discharging mechanism at the interface states may be derived following

Nicollian and Goetberger.[25] In a the case when both acceptor and donor states are present (Case 3 in Sec. III), the responses of the interface states will be determined by the time constants of the corresponding states given by

$$\tau_a = \exp(q\psi_s/kT)/\sigma_a v_{\text{th}} N_D, \tag{21}$$

$$\tau_d = \exp(q\psi_s/kT)/\sigma_d v_{\text{th}} N_D, \tag{22}$$

where $\sigma_{a,d}$ are the capture crossections of the interface states.

The interface state current in such a case can be written as

$$j_{\text{it}} = (G_{\text{it}}^{a,d} + i\omega C_{\text{it}}^{a,d})\,\delta\psi_s, \tag{23}$$

where

$$G_{\text{it}}^{a,d} = q^2 D_{\text{it}}^a/2\tau_a \ln(1+\omega^2\tau_a^2) + q^2 D_{\text{it}}^d/2\tau_d \ln(1+\omega^2\tau_d^2), \tag{24}$$

$$C_{\text{it}}^{a,d} = q^2 D_{\text{it}}^a/\omega\tau_a \arctan(\omega\tau_a) + q^2 D_{\text{it}}^d/\omega\tau_d \arctan(\omega\tau_d). \tag{25}$$

The depletion layer width of the semiconductor undergoes fluctuations in presence of an ac signal across the device. These fluctuations in the depletion layer width cause charging and discharging of the semiconductor space charge region which constitute a current[25]

$$j_{\text{sc}} = i\omega C_{\text{sc}}\delta\psi_s, \tag{26}$$

where $C_{\text{sc}} = (q\epsilon_s N_d/2\psi_s)^{1/2}$ is the depletion layer capacitance.

V. DEVICE ADMITTANCE

The admittance of the device can be obtained from the total ac current across the device given by

$$j = j_t + j_{\text{it}} + j_{\text{sc}}. \tag{27}$$

Equations (20), (23), and (26) may be substituted in to Eq. (27) to obtain j as a function of $\delta\psi_s$

$$j = (qJ_{\text{dc}}/kT + G_{\text{it}} + \iota\omega C_{\text{it}} + \iota\omega C_{\text{isc}})\,\delta\psi_s. \tag{28}$$

Note that the admittance of the device cannot be obtained unless the term $\delta\psi_s$ is expressed in terms ac voltage change, δV.

In order to correlate $\delta\psi_s$ with δV, we evaluate the time derivative of Eq. (4)

$$dQ_{\text{it}}^a/dt + dQ_{\text{it}}^d/dt = -\iota\omega C_{\text{isc}}\delta\psi_s - \iota\omega\delta\psi_s C_i\delta\psi_s + \iota\omega C_i\delta V, \tag{29}$$

where we have substituted $Q_{\text{it}} = Q_{\text{it}}^a + Q_{\text{it}}^d$ and $C_i = \epsilon_i/\delta$.

The left-hand side of Eq. (29) simply represents an interface state current

$$j_{\text{it}} = dQ_{\text{it}}^a/dt + dQ_{\text{it}}^b/dt = (G_{\text{it}} + \iota\omega C_{\text{it}})\,\delta\psi_s. \tag{30}$$

From Eqs. (29) and (30), we get

$$\delta\psi_s/\delta V = \iota\omega C_i/\{G_{\text{it}} + \iota\omega(C_{\text{sc}} + C_{\text{it}} + C_i)\}, \tag{31}$$

where G_{it} and C_{it} are given by Eqs. (24) and (25).

Equations (28) and (31) can be used to obtain the admittance of the contact given by

$$\begin{aligned} Y = j/\delta V &= [\{(J_{\text{dc}})/(kT/q)\} + G_{\text{it}} + \iota\omega(C_{\text{sc}} + C_{\text{it}})]\,\iota\omega C_i/ \\ &\quad \{G_{\text{it}} + \iota\omega(C_{\text{sc}} + C_{\text{it}} + C_i)\} \\ &= G + \iota\omega C, \end{aligned} \tag{32}$$

where G and C represent the conductance and capacitance of the device. Now, separating the real and imaginary part of Eq. (32) we get

$$G = [\{(J_{\text{dc}})/(kT/q)\}C_i(C_{\text{sc}} + C_{\text{it}} + C_i) + C_i^2 G_{\text{it}}]/[(G_{\text{it}}/\omega)^2 + (C_{\text{sc}} + C_{\text{it}} + C_i)^2] \tag{33}$$

and

$$C = [C_i\{(J_{\text{dc}}/(kT/q)\}G_{\text{it}}/\omega^2 + (G_{\text{it}}/\omega)^2 + (C_{\text{sc}} + C_{\text{it}}) \times (C_{\text{sc}} + C_{\text{it}} + C_i) +]/[(G_{\text{it}}/\omega)^2 + (C_{\text{sc}} + C_{\text{it}} + C_i)^2]. \tag{34}$$

It is seen from the above equations that the frequency dependence of G and C will be determined by the terms G_{it}/ω and C_{it}.

VI. EFFECT OF THE INTERFACE REACTION

The interface reaction is particularly important for silicon devices. The reaction takes place between the metal contact and interfacial layer. For example, the reaction between an interfacial SiO_2 layer and a metal-like aluminum readily yields free silicon at the interface.[31] Being tetravalent in nature, the free silicon atoms act as fourfold electron traps. A negative charge density therefore develops at the interface, which tends to increase the barrier height of devices on n-type silicon and reduce it for p-type devices. The barrier modification continues until an equilibrium is reached. As a result, the barrier height becomes dependent on aging time. It is possible that the above mechanism may well cause substantial changes in the current, conductance, and capacitance of the device.

The charge density at free silicon traps liberated in the reaction can be obtained considering rate equation given by[31]

$$Q_{\text{Si}} = qfN_{\text{SiO}_2}\{1 - \exp(-\beta_l t)\}, \tag{35}$$

where β_l is a constant determine the growth of oxide due to reaction of metal with the SiO_2 layer. In the presence of the silicon traps, the charge neutrality equation can be written in a modified form by including a charge density due to free silicon at the interface given by

$$Q_m + Q_{\text{sc}} + Q_{\text{it}} + Q_f + Q_{\text{si}} = 0. \tag{36}$$

Equations (35) and (36) along with Eqs. (2), (3), (5), and (15) give the dependence of surface potential on aging time given by

$$\begin{aligned} \psi_s(t) = \psi_{ad}(t)/\{&C_{2d} + (1 - C_{2d})C_{2a}\} \\ &+ C_{2a}^2 C_{2d}^2 C_1/[2\{C_{2d} + (1 - C_{2d})C_{2a}\}]^2 \\ &- [4C_{2a}^2 C_{2d}^2 C_1 \psi_{ad}(t)\{C_{2d} + (1 - C_{2d})C_{2a}\} \\ &+ C_{2a}^4 C_{2d}^4 C_1^2]^{1/2}/[2\{C_{2d} + (1 - C_{2d})C_{2a}\}],^2 \end{aligned} \tag{37}$$

where

$$\psi_{ad}(t)=C_{2a}C_{2d}(\phi_m-\chi)+(1-C_{2a})C_{2d}E_g - qC_{2a}C_{2d}\delta N_f/\epsilon_i-\{C_{2d}+(1-C_{2d})C_{2a}\} \times V_n-C_{2a}C_{2d}V+C[1-\exp(-\beta_l t)], \quad (38)$$

where $C=4qfC_{2a}C_{2d}\delta N_{\mathrm{SiO}_2}(0)/\epsilon_i$, N_{SiO_2} the density of SiO_2 molecules per cm^2, f is a parameter that determines the maximum value of the charge density at the silicon traps. The value of C for an Al–SiO_2–p-Si system has been found by a method of fitting to be 0.25 eV. It may be noted that the surface potential becomes dependent on aging time through Eq. (38) and consequently, all the quantities J_{dc}, G_{it}^{ad}, C_{it}^{ad}, C_{sc}, C, and G are all functions of aging time. It is possible to obtain simplified expressions for the above quantities under the condition of low or moderate values of the doping concentration and very thin interfacial layer. In such cases, the surface potential can be approximated as

$$\psi_s(t)=\psi_{ad}+C[1-\exp(-\beta_l t)]. \quad (39)$$

With the help of Eq. (39), one obtains

$$J_{\mathrm{dc}}=J_{\mathrm{dc}}(0)/\gamma(t), \quad (40)$$

$$\tau_a=\tau_a(0)\gamma(t), \quad (41)$$

$$\tau_d=\tau_d(0)\gamma(t), \quad (42)$$

$$G_{\mathrm{it}}=[q^2D_{\mathrm{it}}^a/\{2\tau_a(0)\gamma(t)\}]\ln[1+\omega^2\tau_a(0)^2\gamma(t)^2] +[q^2D_{\mathrm{it}}^d/\{2\tau_d(0)\gamma(t)\}]\ln[1+\omega^2\tau_d(0)^2\gamma(t)^2], \quad (43)$$

$$C_{\mathrm{it}}^{a,d}=[q^2D_{\mathrm{it}}^a/\omega\tau_a(0)\gamma(t)]\arctan\{\omega\tau_a(0)\gamma(t)\} +[q^2D_{\mathrm{it}}^d/\omega\tau_d(0)\gamma(t)]\arctan\{\omega\tau_d(0)\gamma(t)\}, \quad (44)$$

$$C_{\mathrm{sc}}=[q\epsilon_s N_d/[2\{\psi_{ad}(t)+C-C\exp(-\beta_l t)\}]]^{1/2}, \quad (45)$$

$$\gamma(t)=\exp[qC\{1-\exp(-\beta_l t)\}], \quad (46)$$

where $\tau_{a,d}(0)$ are the time constants for acceptor and donor states at time $t=0$.

The above equations can be substituted in Eqs. (33) and (34) to obtain the dependence of the conductance and capacitance on aging time. However, in the present case, instead of studying the aging behavior with the help of the above approximate equations, Eq. (37) has been used for generality and the salient features of aging on the surface potential, dc tunnel current, interface state time constants, interface state capacitance and conductance, and the total device capacitance and conductance have been investigated. The results are illustrated in Figs. (2)–(11). In all these figures, the aging characteristics are represented by broken line curves corresponding to a time $t=10^4$ s and those before aging (corresponding to time $t=0$) have been represented by continuous line curves.

VII. DISCUSSIONS

The presence of interface states of different varieties, namely, the donor, acceptor, and donor–acceptor mixed states influence the device characteristics in many ways. First of all, the surface potential of the device gets modified. The donor states tend to reduce the potential as these states yielding a positive charge density develops at the interface. Acceptor states on the contrary yield negative charge density and thereby increase the surface potential. When the two types of states are present simultaneously, the surface potential will be determined by the dominance of any of the two kinds of states, donors or acceptors. The situations are illustrated in Fig. 2. It is seen from the figure that, though the slope of ψ_s vs V plot remain almost the same for acceptor or donor states, it decreases when both the donors and acceptors are present simultaneously. What seems to be more interesting is that these plots shift with time due to interface reaction. The change in surface potential caused by the above effect is additive for devices on n-type semiconductors and predominantly determined by the constants C and β_l. The larger the value of β_l, the faster will be the change of Ψ_s with time. The constant C on the other hand determines the maximum change that may be caused by the interface reaction.

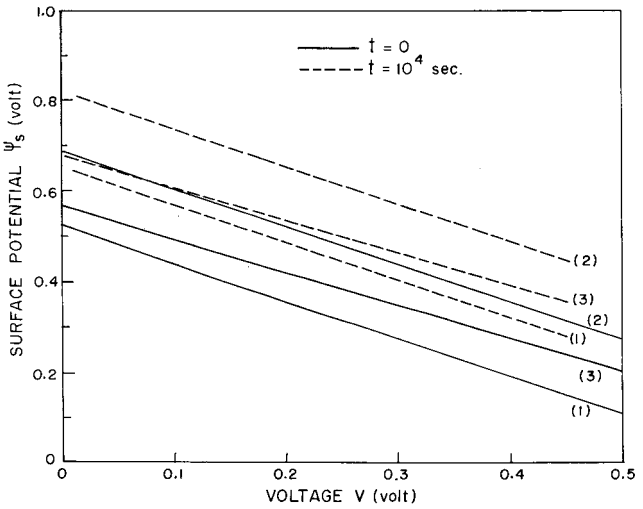

FIG. 2. Variation of surface potential ψ_s of a MIS tunnel contact as a function of bias voltage in the presence of interface states and interface reaction. Parameters: $\phi_m=5.1$ eV, $\delta=10$ Å and $N_D=10^{15}\,\mathrm{cm}^{-3}$. Curves (1,1): $D_{\mathrm{it}}^d=5\times10^{11}\,\mathrm{cm}^{-2}\,\mathrm{eV}^{-1}$, $D_{\mathrm{it}}^a=0$. Curves (2,2): $D_{\mathrm{it}}^d=0$, $D_{\mathrm{it}}^a=10^{12}\,\mathrm{cm}^{-2}\,\mathrm{eV}^{-1}$. Curves (3,3): $D_{\mathrm{it}}^d=5\times10^{11}\,\mathrm{cm}^{-2}\,\mathrm{eV}^{-1}$, $D_{\mathrm{it}}^a=10^{12}\,\mathrm{cm}^{-2}\,\mathrm{eV}^{-1}$. Broken line curves represent the variation after an aging time $t=10^4$ s.

An immediate consequence of the modification of the surface potential is reflected in the current–voltage characteristics. The current density is higher for the lower values of surface potential. Thus, the reduction in the surface potential due to donor states is the cause for the increase in the current density in Fig. 3. However, since the acceptor states increase the surface potential, the current density is reduced. In the presence of the donor–acceptor composite, the current density attains an intermediate value. But noticeably, in the case of mixed interface, the slope of the logarithmic current density versus voltage plot is different from the former two cases when either the donor or acceptor states are present. This nature of variation remains the same even after aging. However, the current values change quite significantly with aging time $t=10^4$ s., the current–voltage characteristics (broken

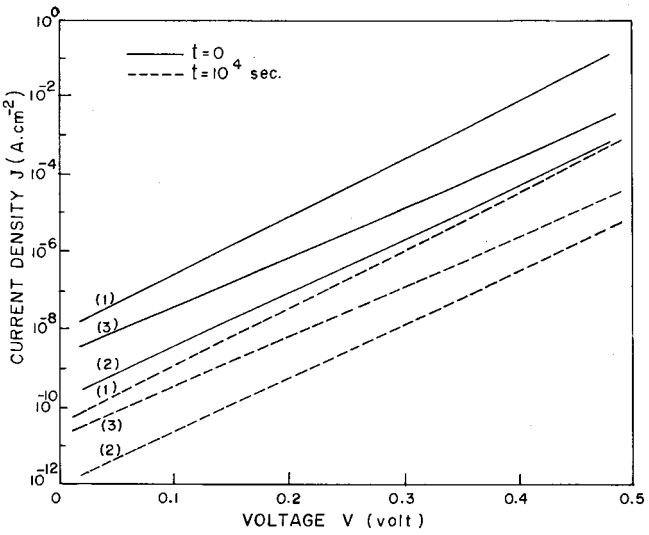

FIG. 3. Current–voltage characteristics of a MIS tunnel contact in the presence of interface states and the interface reaction. Parameters: $\phi^{1/2}\delta=2$, $A=120\ \mathrm{A\,cm^{-2}\,K^{-2}}$, and $T=300$ K. The values of the other parameters including those for curves (1,1), (2,2), and (3,3) are same as in Fig. 2.

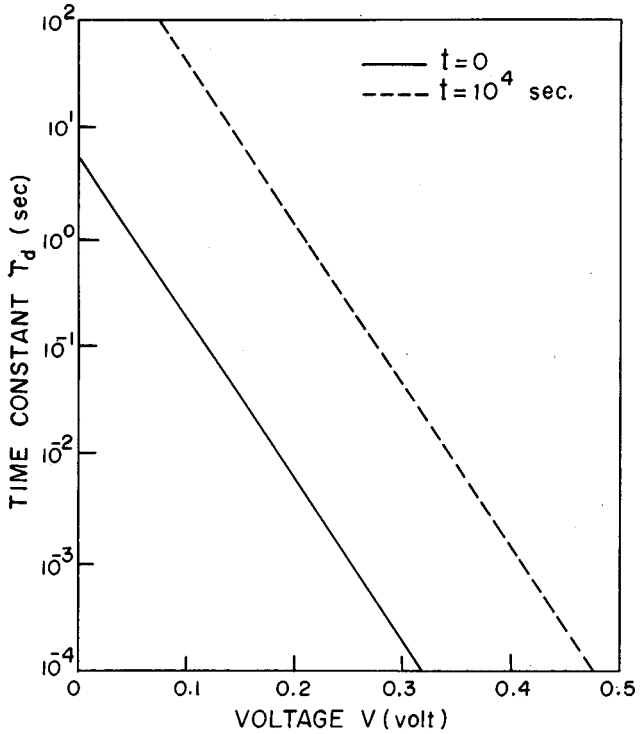

FIG. 4. Variation of time constant τ_d of donor-like interface states as a function of applied voltage in the presence of interface reaction. Parameters: $\sigma_d=10^{-13}\ \mathrm{cm^2}$, $v_{\mathrm{th}}=10^7\ \mathrm{cm\,s^{-1}}$, and $D_{\mathrm{it}}^d=5\times10^{11}\ \mathrm{cm^{-2}\,eV^{-1}}$. The values of the other parameters are same as those in Fig. 2. The nature of variation after aging time $t=10^4$ s is shown by broken line.

line curves) are shifted parallel upward causing considerable change in the device current. This shows the significance of the aging effect originating from the interface reaction.

The ac behavior of the device is primarily determined by the ability of the interface states to follow the applied signal. This can be described by the time constant of the states. According to Eqs. (21) and (22), the time constant of the interface states is a function of surface potential besides other parameters namely the capture cross section, doping concentration, and temperature. The voltage dependence of the time constant comes through the voltage dependence of the surface potential. In Figs. 4 and 5, the logarithmic values of the time constants are plotted as a function of voltage. Interestingly the time constant of the states becomes sensitive to the aging time. As typical examples, the shifting in the values of the time constant for donor and acceptor states after an aging time $t=10^4$ s have been shown in the above figures (broken line curves). Such a change in the time constant suggest interface states to respond at frequencies different from the case when $t=0$.

The conductance–voltage characteristics of the device show a variety of features. These plots show linear or a step-like variation depending upon the response of the interface states. For given values of the applied bias, interface state density, capture cross section, and the surface potential, a particular type of state may be operative and yield excess conductance due to the interface states. Consequently, the total conductance deviates from the linearity. Also shown in the figure is how the interface states of different kinds can bring in striking effects in the conductance plots of the device. The conductance values are further influenced due to the aging of the device. The effect of aging on the device conductance has been illustrated in the same figure after the device undergoes an aging processes for a time $t=10^4$ s. In all these three cases of acceptors, donors, or acceptor–donor mixed interfaces, the effect of aging leads to considerable

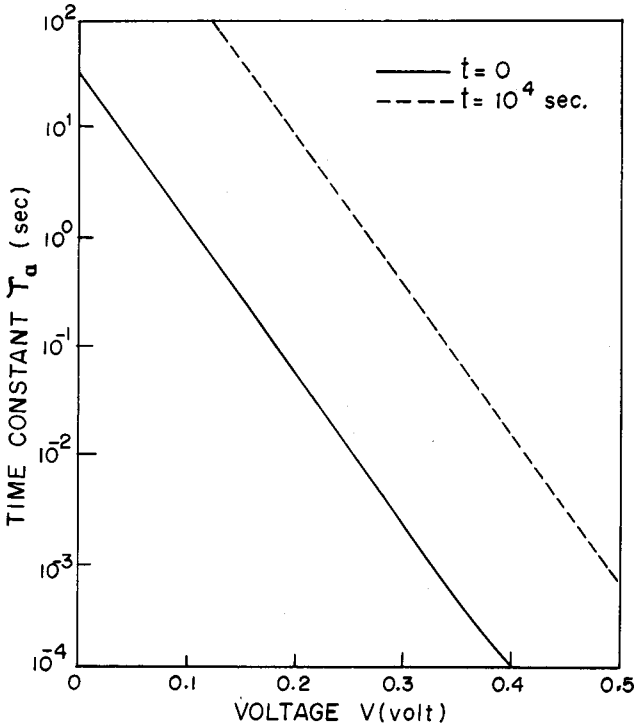

FIG. 5. Variation of time constant τ_a of acceptor-like interface states as a function of applied voltage in the presence of interface reaction. Parameters: $\sigma_a=10^{-12}\ \mathrm{cm^2}$, $v_{\mathrm{th}}=10^7\ \mathrm{cm\,s^{-1}}$, and $D_{\mathrm{it}}^a=5\times10^{11}\ \mathrm{cm^{-2}\,eV^{-1}}$. The values of the other parameters are same as those in Fig. 2. The Nature of variation after aging time $t=10^4$ s is shown by broken line.

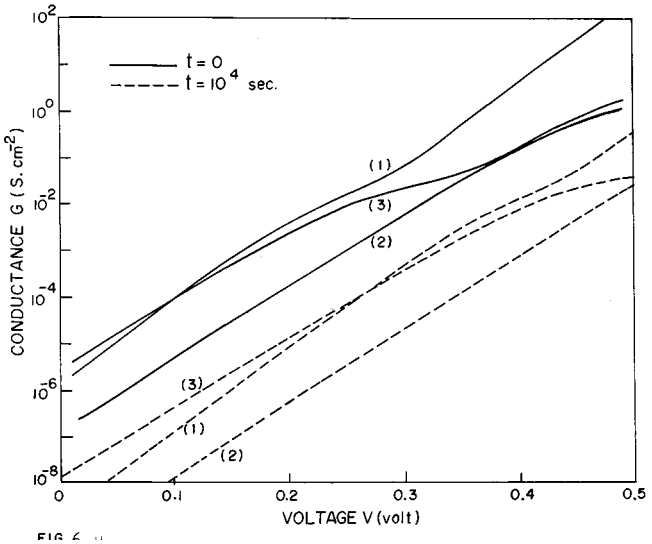

FIG. 6. The variation of ac conductance of a MIS tunnel device as a function of bias voltage in the presence of interface states and interface reaction. Parameters: $\sigma_a = 10^{-12}\,\mathrm{cm}^2$, $\sigma_d = 10^{-14}\,\mathrm{cm}^2$, and $v_{\mathrm{th}} = 10^7\,\mathrm{cm\,s}^{-1}$. The values of the other parameters including those for curves (1,1), (2,2), and (3,3) are same as those in Fig. 2. The variation after a time $t = 10^4$ s of the aging device is shown by broken line curves.

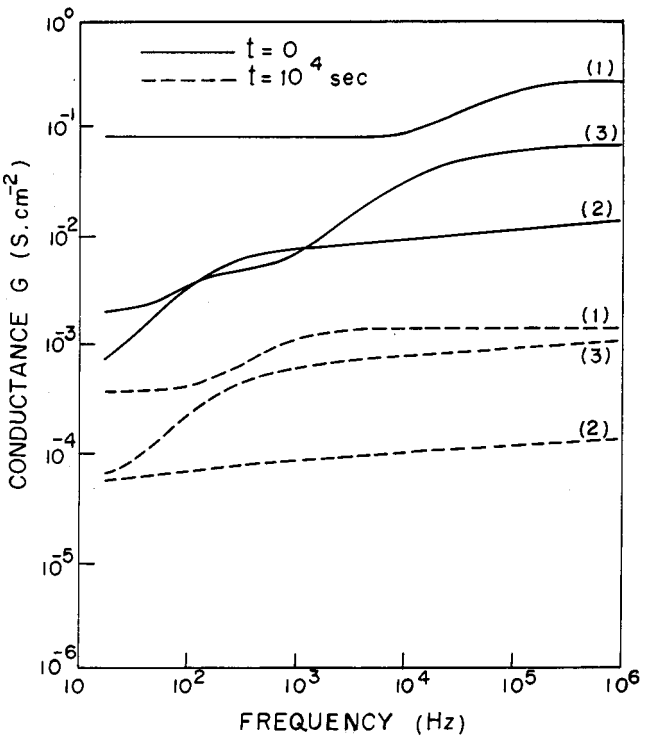

FIG. 7. The variation of ac conductance of a MIS tunnel device as a function of frequency of the applied ac signal in the presence of interface states and interface reaction. Parameters: $\sigma_a = 10^{-12}\,\mathrm{cm}^2$, $\sigma_d = 10^{-14}\,\mathrm{cm}^2$, and $v_{\mathrm{th}} = 10^7\,\mathrm{cm\,s}^{-1}$. The values of the other parameters including those for curves (1,1), (2,2), and (3,3) are same as those in Fig. 2. The variation after an aging time $t = 10^4$ s are shown by broken line curves.

reduction in the conductance values. Such a reduction may be realized in terms of modification of the surface potential of the device as a consequence of interface reaction. Note that the conductance step, which appears at a particular voltage, shifts to the higher voltage as the device undergoes the aging effect. The shift is caused by the change in the time constant of the device with aging time. (Also see Fig. 6.)

Figure 7 illustrates the frequency dispersion of the conductance over the range $10-10^7$ Hz. In this case the conductance steps in the frequency domain result from the charging and discharging of interface states in presence of the ac signals. The density and the time constant of the interface states determine the step height and the frequency at which a particular step occurs. The interface states start responding to the ac signal when the inverse of the frequency matches with the time constant of the states. This will be determined by the applied voltage since the time constant of the interface states is voltage dependent through the term surface potential. As the voltage increases, the values of Ψ_s decreases and consequently, the value of τ decreases causing a shift of the conductance values towards the higher side of the frequency scale. It may be noted that the two conductance steps appearing in the figure (curve 3 for $t = 0$) correspond to two types of states. One of these states corresponds to a low value of time constant while the other appears for states having a larger value of time constant. After aging for time $t = 10^4$ s, the conductance values are considerably reduced. Note that the two conductance steps found before aging (corresponding to mixed interface having donors and acceptor both) is now reduced to single steps (broken line curve 3). The reason for the disappearance of one of the steps is solely due to the increase in the value of the corresponding time constant due to aging. The appearance of the missing conductance step expected to appear at the lower frequency not shown in the above figure. It may be mentioned further, that closer to the values of $D_{\mathrm{it}a}$, $D_{\mathrm{it}d}$, τ_a, and τ_d of the two variety of states, the responses would occur almost at the same frequency and the two conductance steps tends to merge leading a single step in the conductance plot.

The capacitance voltage characteristics of the device are shown in Fig. 8. In general, the capacitance increases with forward voltage until it assumes a constant value corresponding to the capacitance of the interfacial layer. Such a variation is true for any type of the states, acceptors or donors. But, when both types of states are present simultaneously, capacitance varies in steps with bias voltage. The step-like variation occurring at lower voltage is due to acceptor states while the similar variation at comparatively higher voltage is related to donor states. The values of the capacitance at the steps are determined by the respective density and time constant of the states. As a consequence of the interface reaction, the shifting of the $C-V$ curves occurs with time. Such dependence can be understood in terms of modifications in the values of the surface potential and the time constant of the states. The increase in the surface potential decreases the depletion layer capacitance, while the increase in the time constant leads the interface state response to occur at the relatively lower frequencies. Because of the presence of two types of states of different time constants, the responses occur at two different frequencies.

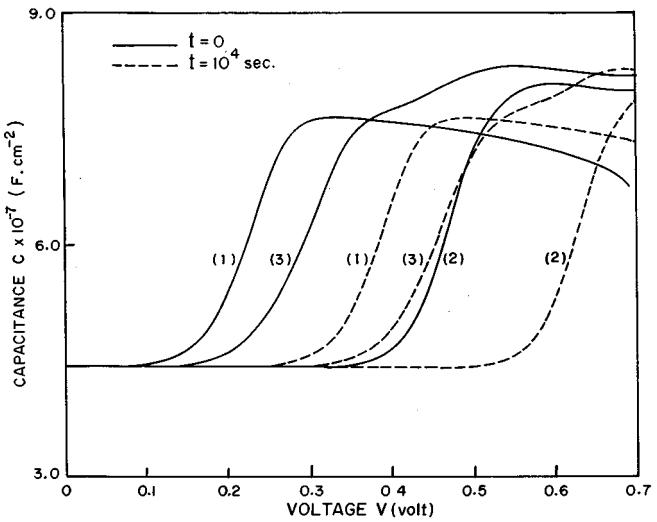

FIG. 8. The capacitance–voltage characteristics of a MIS tunnel device as a function of bias voltage in the presence of interface states and interface reaction. Parameters: $\sigma_a = 10^{-12}\,\mathrm{cm}^2$, $\sigma_d = 10^{-14}\,\mathrm{cm}^2$, and $v_{\mathrm{th}} = 10^7\,\mathrm{cm\,s}^{-1}$. The values of the other parameters including those for curves (1,1), (2,2), and (3,3) are same as those in Fig. 2. The variations after a time $t = 10^4$ s are shown by broken lines.

Figure 9 shows the frequency dependence of the device capacitance. It is seen from the figure that the capacitance decreases with the frequency until it becomes saturated at very high frequency. The value of the capacitance at high frequency corresponds purely to the depletion layer capacitance of the device. At these frequencies, the interface states cannot follow the ac signal. The response from the interface states only appears at relatively lower frequencies. As it is seen from the figure, the capacitance assumes maximum value at very low frequencies when the interface states follow the applied signal. In presence of single type of states (either donor or acceptor), the capacitance versus frequency plot show a capacitance step. But, when both the donor and acceptor states are present, an additional step appears. Thus, the existence of a capacitance step is correlated to a particular type of state. The frequencies where these steps occur will be determined by the time constants of the states. Of course, as evident from the functional dependence τ, parameters such as the capture cross section, doping, and surface potential will actually fix the time constant and hence the frequency at which a particular type of state responds under ac conditions. Whether a capacitance step is observable or not will be determined by the density of states. The higher the value of the interface state density, the larger the low frequency capacitance will be. Moreover, these plots can be readily influenced due to interface reaction. In the presence of interface reaction, the value of capacitance changes with time. Illustrated in the same figure, how the capacitance of the device changes after an aging time $t = 10^4$ s. It may be noted that all the curves are shifted considerably compared to those for $t = 0$. The value of the rate constant β_l determine how fast such a shift will occur and the constants C will determine the maximum shift that can be observed due to interface reaction.

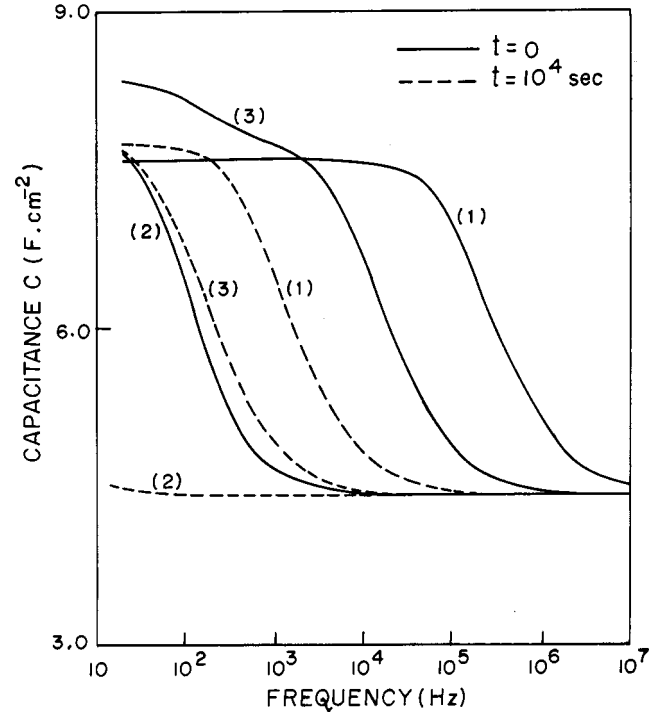

FIG. 9. The variation of the capacitance of a MIS tunnel device with the frequency of the applied ac signal in the presence of interface states and interface reaction. Parameters: $\sigma_a = 10^{-12}\,\mathrm{cm}^2$, $\sigma_d = 10^{-14}\,\mathrm{cm}^2$, and $v_{\mathrm{th}} = 10^7\,\mathrm{cm\,s}^{-1}$. The values of the other parameters including those for the curves (1,1), (2,2), and (3,3) are same as those in Fig. 2. The broken line curves represent the variation after the aging time $t = 10^4$ s.

The presence of the donor–acceptor mixed interface and the interface reaction may have significant effect on various techniques that characterize the interface states. For example, well known admittance spectroscopy for the determination of the density and capture cross section of the interface states may lead to several misleading conclusions particularly for aging devices. Usually, for the purpose of determining the interface state parameters, the interface state conductance of the device is extracted from the measured values of the device conductance and from a plot of G_{it}/ω vs ω, the interface state density and the time constants are determined. If the interface reaction is disregarded then the above extraction procedure may lead to a wrong conclusion that some other interface parameters are changing with time. As illustrated in this work, the main reason for the time evolution of the conductance plot is, however, the interface reaction typical for the aging devices. For further illustration, it is shown in Fig. 10 how the G_{it}/ω vs ω plot may change with aging time. Also shown in the same figure is the effects of the presence of the two variety of states, acceptors and donors. The existence of these states yield two definite peaks, one corresponds to acceptor and the other donor states. The presence of such peaks has been observed in many experiments. Losee[26,27] observed two peaks in the above plot and attributed them to interface and bulk defect states, respectively. The present study, however, demonstrates other possibilities to interpret similar results namely, by considering the donor–acceptor composite interface. It may be mentioned that, in the case of interface states having specific energy distribution

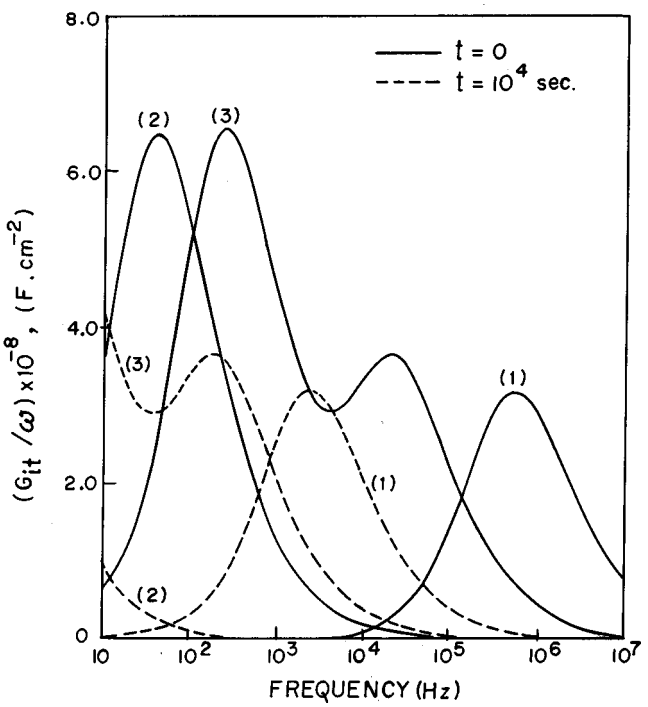

FIG. 10. The G_{it}/ω vs ω plot of MIS tunnel contact in the presence of interface reaction. Parameters: $\sigma_a = 10^{-12}\,\mathrm{cm}^2$, $\sigma_d = 10^{-14}\,\mathrm{cm}^2$, and $v_{th} = 10^7\,\mathrm{cm\,s}^{-1}$. The values of other parameters including the parameters for curves (1,1), (2,2), and (3,3) are same as those in Fig. 2. The dashed line plots represent variation after aging for time $t = 10^{-4}$ s.

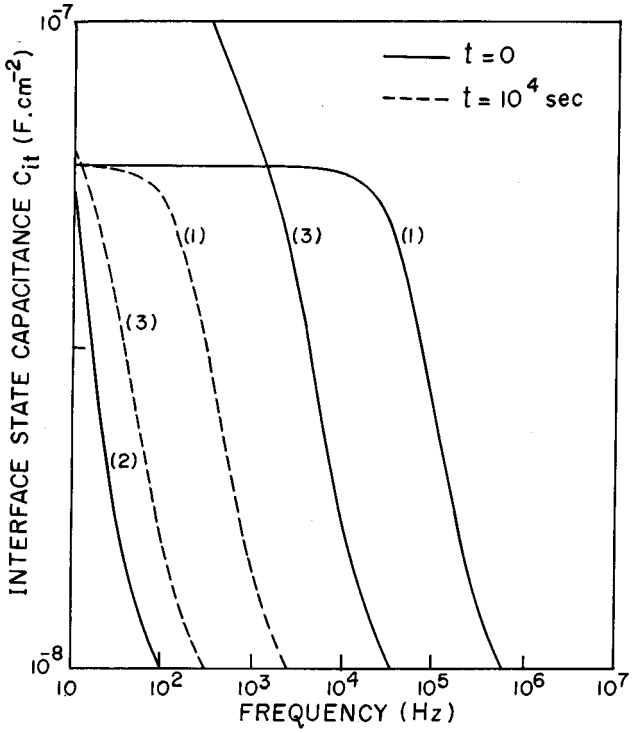

FIG. 11. The variation of interface state capacitance of a MIS tunnel device as a function of bias voltage and interface reaction. Parameters: $\sigma_a = 10^{-12}\,\mathrm{cm}^2$, $\sigma_d = 10^{-14}\,\mathrm{cm}^2$, and $v_{th} = 10^7\,\mathrm{cm\,s}^{-1}$. The values of the other parameters including those for curves (1,1), (2,2), and (3,3) are same as those in Fig. 2. The variation after a time $t = 10^4$ s are represented by broken line curves.

of density of states, the height of the conductance peak will increase with increasing voltage. This is in contrast to bulk states, the conductance peak, of which in most cases, does not increase with applied voltage.

The interface states are also studied by extracting the interface state capacitance from the measured values of the device capacitance. The main features of the variation of interface state capacitance with frequency are shown in Fig. 11. At lower frequencies, the capacitance has been found considerably large due to the ability of the interface states to follow the ac signal. The capacitance values are much lower for the donor states compared to acceptor states or acceptor–donor combination. The relative difference in the values of this capacitance is due to the density of interface states, which is considered to be larger for the acceptor states. The curves (3,3) show the dominance of acceptor states over the donors. In this case the capacitance has also been found to change quite significantly due to the interface reaction for a time 10^4 s. The dashed line curves represent the shift of the capacitance values resulting from the aging process caused by interface reaction.

VIII. CONCLUSION

In conclusion, the admittance model for a MIS tunnel diode has been extended in the case of donor–acceptor mixed interface and interface reaction at the metal–semiconductor interface. The model reveals a number of interesting features. It predicts step-like capacitance and conductance variation with respect to frequency and applied dc bias. A two step variation of the device conductance with frequency limits the application of conventional admittance models based on the consideration of single type of interface states. The analysis therefore applies to generalized surface condition. The proposed model can be readily converged to the basic model on admittance when the density of donor states is set to zero. A striking feature of the analysis of the ac response is the aging behavior of the electrical characteristics of the device. The aging effect is caused by the interface reaction. Because of this effect the surface potential and tunnel current density of the device changes considerably with aging time. The process of aging also makes the time constant of the interface states to be a function of aging time. Such a dependence of the time constant has a remarkable effect on the ac properties of the device, as it has been shown that due to the above effect the device conductance and capacitance become a function of aging time.

ACKNOWLEDGMENTS

The author gratefully acknowledges the All India Council For Technical Education, New Delhi for financial and technical support.

[1] J. Bardeen, Phys. Rev. **71**, 717 (1947).
[2] C. A. Mead and N. G. Spitzer, Phys. Rev. **134**, A713 (1964).
[3] A. M. Cowley and S. M. Sze, J. Appl. Phys. **36**, 3212 (1965).
[4] M. J. Turner and E. H. Rhoderick, Solid-State Electron. **11**, 291 (1968).
[5] A. C. Card and E. H. Rhoderick, J. Phys. D **4**, 1589 (1971).
[6] C. Barret and A. Vapaille, Solid-State Electron. **18**, 25 (1975).
[7] H. C. Card, IEEE Trans. Electron Devices **ED-23**, 538 (1976).

[8] D. L. Pulfrey, IEEE Trans. Electron Devices **ED-23**, 587 (1976).
[9] V. Kumar and W. E. Dahlke, Solid-State Electron. **20**, 143 (1977).
[10] S. Ashoke, J. M. Borrego, and R. J. Gutman, Solid-State Electron. **22**, 621 (1979).
[11] J. T. Lue, Solid-State Electron. **23**, 263 (1980).
[12] A. N. Daw, A. K. Dutta, and M. C. Ash, Solid-State Electron. **25**, 431 (1982).
[13] C. Barret, F. Chekir, and A. Vapaille, J. Phys. C **16**, 2421 (1983).
[14] S. J. Fonash, J. Appl. Phys. **54**, 1966 (1983).
[15] P. Chattopadhyay and A. N. Daw, Solid-State Electron. **29**, 555 (1986).
[16] J. H. Werner, *Metallization and Metal-Semiconductor Interfaces* (Plenum, New York, 1989), p. 235.
[17] P. Chattopadhyay and B. Raychaudhuri, Solid-State Electron. **36**, 605 (1993).
[18] P. Chattopadhyay, Solid-State Electron. **37**, 1759 (1994).
[19] P. Chattopadhyay, Solid-State Electron. **39**, 1491 (1996).
[20] V. Heine, Phys. Rev. A **138**, 1689 (1965).
[21] S. G. Louie and M. L. Cohen, Phys. Rev. B **13**, 2461 (1976).
[22] W. Monch, J. Vac. Sci. Technol. B **6**, 1270 (1988).
[23] W. De. Bosscher, R. L. Van Meirhaeghe, A. De. Laere, W. H. Laflere, and F. Cardon, Solid-State Electron. **31**, 945 (1988).
[24] R. L. Meirhaeghe, L. M. O. Van Den Berge, W. H. Laflere, and F. Cardon, Solid-State Electron. **31**, 1629 (1988).
[25] E. H. Nicollian and A. Goetzberger, Bell Syst. Tech. J. **46**, 1055 (1967).
[26] D. L. Losee, Appl. Phys. Lett. **21**, 54 (1972).
[27] D. L. Losee, J. Appl. Phys. **46**, 2204 (1975).
[28] K. M. Brunson, D. Sands, C. B. Thomas, and H. S. Reehai, J. Appl. Phys. **62**, 185 (1987).
[29] M. H. Yayarani-Najaran, D. Sands, K. M. Brunson, and C. B. Thomas, J. Appl. Phys. **67**, 1980 (1990).
[30] E. H. Rhoderick and R. H. Williams, *Metal-Semiconductor Contacts*, 2nd ed. (Clarendon, Oxford, 1986), p. 54.
[31] P. Chattopadhyay and K. Das, J. Appl. Phys. **80**, 4229 (1996).
[32] P. Chattopadhyay, Appl. Surf. Sci. **126**, 65 (1998).
[33] P. Chattopadhyay, J. Phys. D **31**, 1060 (1998).
[34] P. Chattopadhyay, International Conference on Silica Science and Technology, Mulhouse, France, 1–4 September, 1998, p. 411.